Accumulations and Equilibrium Conditions of Organophosphate Esters (OPEs) in the Indoor window film and the estimation of concentrations in Air

Chun-Yan Huo[a,b,c], Li-Yan Liu[a,b,c*], Hayley Hung[e], Yu Sun[a,b,c], Jia-Qi Guo[a,b,c], Yong-Kai Wu[a,b,c], Ed Sverko[a,b,c,], and Wen-Long Li[d,e]

[a] International Joint Research Center for Persistent Toxic Substances (IJRC-PTS)/International Joint Research Center for Arctic Environment and Ecosystem (IJRC-AEE), State Key Laboratory of Urban Water Resource and Environment, Harbin Institute of Technology, Harbin 150090, China

[b] School of Environment, Harbin Institute of Technology, Harbin 150090, China

[c] University Corporation for Polar Research, Beijing 100875, China

[d] College of the Environment and Ecology, Xiamen University, Xiamen, PR China

[e] Air Quality Processes Research Section, Environment and Climate Change Canada, 4905 Dufferin Street, Toronto, Ontario M3H 5T4, Canada

Word count: (Text) 5750 + 1 (Table) × 300 + 3 (Figure) × 300 = 6950, including text, tables and figures**.**

*Corresponding authors. Li-Yan Liu, International Joint Research Center for Persistent Toxic Substances, State Key Laboratory of Urban Water Resource and Environment, Harbin Institute of Technology, Harbin 150090, China; E-mail: llyan7664@163.com.

Graphical Abstract:

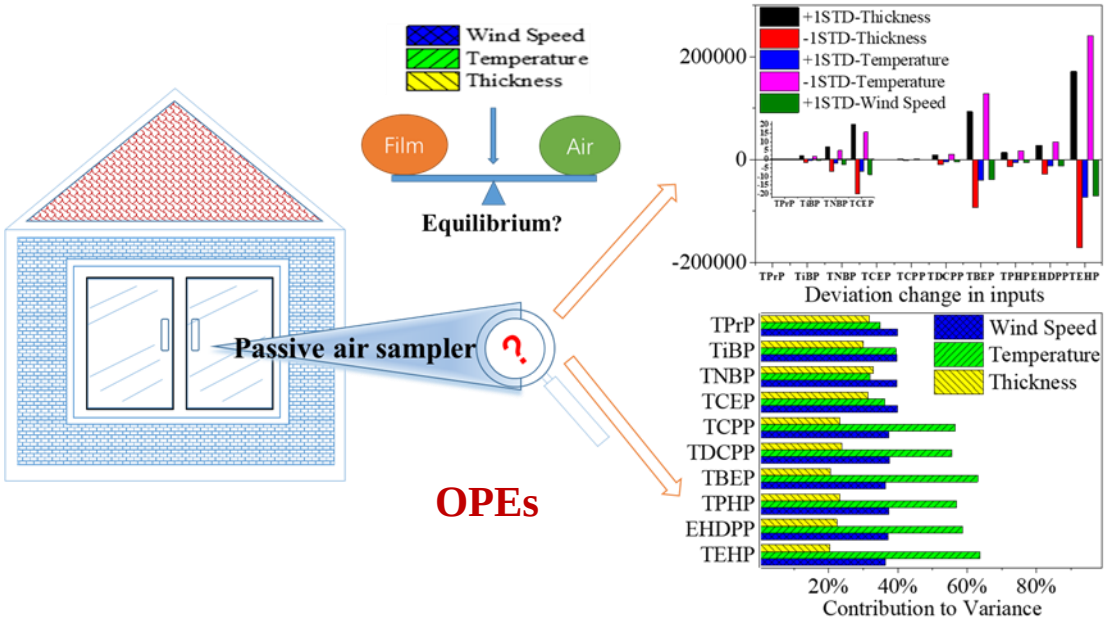

Highlights

- Organophosphate esters (OPEs) in window films exhibited linear growth patterns
- Temperature, humidity, ventilation, and seasonality all affected the concentrations of OPEs
- Most lower mass OPEs stay in the indoor air because of their short equilibrium time
- Equilibrium time of OPEs reveals the variability in the fates of OPEs in the indoor environment

ABSTRACT: The study of the fate of organophosphate esters (OPEs) in the interior environment is vital because of the growing use of OPEs. Organic films on glass are both sink and sources of indoor pollutants. Indoor window films have been employed as passive air samplers to collect OPEs in the indoor air. Nevertheless, little is known about the development and equilibrium condition of OPEs on indoor window films during the film formation process. In this study, the concentrations of twelve OPEs in indoor window films from different buildings on a university campus and the growth thickness of the films as a function of sampling time were investigated in different seasons. Ten out of the 12 OPEs were detected in window film with >50% frequency. Tris (2-chloroethyl) phosphate (TCEP) and tris (1-chloro-2-propyl) phosphate (TCPP), which are chlorinated and toxic OPEs, were the dominant OPEs found in the winter. The majority of OPEs in window films exhibited linear growth patterns within 77 days. Temperature, humidity, ventilation, and seasonality all affected the concentrations of various OPEs in the window films. Low molecular weight OPEs, such as tri-n-butyl phosphate and TCEP, attained equilibrium between indoor air and window films within 49 or 77 days. The indoor air concentrations of OPEs were estimated from their film concentrations based on the theoretical approach for the passive air sampler. In winter, the predicted gas-phase air concentrations of OPEs (3.7 ng/m^3 for TECP) were significantly lower than or comparable to summer (11 ng/m^3, $p < 0.05$). To the best of our knowledge, this is the first attempt to combine uncertainty and sensitivity analysis to understand the behaviors of OPEs in indoor film and air.

Keywords: Indoor Film, OPEs, Equilibrium Time, Passive Air Sampler

1. Introduction

Organophosphate esters (OPEs) are a group of flame retardants and plasticizers widely used in polyurethane foam (PUF), furniture, plastics, textiles, electronic equipment, and food-wrapping film (Wei et al., 2015, Shoeib et al., 2019). With the phasing out of polybrominated diphenyl ethers (PBDEs), the production of OPEs has increased and accounted for 30% of the total global flame retardant demands in 2013 (Shoeib et al., 2019). OPEs can leach into the environment through abrasion, dissolution, and volatilization (Kemmlein et al., 2003). OPEs were widely found in the atmosphere (Zhang et al., 2019), seawater (Hu et al., 2014), sediment (Zhong et al., 2018), indoor air (Kim et al., 2019), dust (Shoeib et al., 2019), window film (Vykoukalova et al., 2017, Persson et al., 2018), biota (Hallanger et al., 2015), human breast milk (Kim et al., 2014), and remote regions including the North Atlantic and Arctic (Suhring et al., 2016, Li et al., 2017).

On a regular basis, humans are exposed to OPEs through inhalation, ingestion, and dermal contact. Recent risk assessments of OPEs confirmed their harmful impacts on human health, including carcinogenic, teratogenic, neurotoxic, and metabolic toxicity (Greaves and Letcher 2017). There are significant concerns regarding chlorinated OPEs, of which tris (1-chloro-2-propyl) phosphate (TCPP) and tris (1,3-dichloro-2-propyl) phosphate (TDCPP) have been linked to carcinogenic effects (Ni et al., 2007); and tris (2-chloroethyl) phosphate (TCEP) has been linked to adverse health effects of hemolysis and reproduction (Zhang et al., 2019). Non-chlorinated OPEs such as triphenyl

77 phosphate (TPHP) have been demonstrated to disrupt hormone levels and lower male
78 sperm quality (Meeker and Stapleton 2010).
79 Pollution in the indoor environment is an important factor affecting human health
80 because humans usually spend around 90% of their time indoors (Mitra and Ray 1995).
81 The window film can be considered a dynamic absorption model to collect both gas-
82 phase and particle-phase air pollutants for a given period. Window films being
83 oily/sticky in nature, especially on the floor-to-ceiling windows, would also capture fine
84 particles that could be suspended in the indoor air with walking or other indoor activities.
85 The window film accumulates various types of organic contaminants, including
86 polycyclic aromatic hydrocarbons (PAHs) (Terzaghi et al., 2015), phthalates (PAEs)
87 (Huo et al., 2016), polychlorinated biphenyls (PCBs) (Wu et al., 2008), PBDEs (Cetin
88 and Odabasi 2011), and OPEs (Vykoukalova et al., 2017).
89 Window films are typically quite a relevant part of indoor fate models, which can
90 provide a valuable understanding that can help better parameterize models. Recently
91 published articles on the equilibration time of Semi-Volatile Organic Compounds
92 (SVOCs) in window film mainly focused on the influence of octanol-air partition
93 coefficients (K_{OA}). Weschler et al. established a model which predicted that SVOCs with
94 lower log K_{OA} values (in the range of 10-13) would equilibrate between the gas phase
95 and the surface film more quickly (Weschler and Nazaroff 2017). Li et al. proposed that
96 SVOCs with log K_{OA} less than eight or greater than 11 were not at the equilibrium state
97 between air and window films (Li et al., 2019). Vykoukalova et al. suggested that OPEs

with log K_{OA} less than 12 can reach equilibrium between air and window films (Vykoukalova et al., 2017). In our previous study, the time required to reach equilibrium was calculated for PAH, which showed that when the window film is thinner (4 nm), a shorter equilibration time (<7 days) was required for PAHs with a lower log K_{OA} of less than 10.6 (Huo et al., 2019).

Based on the passive air sampler (PAS) theory, Terzaghi et al. converted PAH concentrations in the outdoor window films into atmospheric concentrations, with the equilibration times calculated using measured temperature, wind speed, and other parameters (Terzaghi et al., 2015). However, there is a lack of sensitivity and uncertainty analyses on modeling the equilibrium time of SVOCs in window film. The equilibrium conditions of OPEs in the indoor window film and the utility of the window film as a passive sampler for OPEs are not well studied. As with other SVOCs, the role of the indoor window film in the distribution of OPEs could be crucial. Therefore, the objectives of this study are (a) to investigate the accumulative characteristics of OPEs in window films; (b) to estimate the equilibrium time between window film and air; (c) to explore the sensitivity and uncertainty of estimating the equilibrium time which was related to film thickness, log K_{OA}, and wind speeds; (d) to convert the gas-phase air concentrations of OPEs from window film; and (e) to understand the suitability of window film as a PAS for OPEs.

2. Materials and methods

2.1. Sample collection and analysis

The collection and extraction of film samples have been described in previously published articles (Huo et al., 2016, Huo et al., 2019). A detailed description of the sampling site can be found in Supporting Information (SI) Table S1. The sampling campaign was performed weekly in winter (N = 26) and summer (N = 38) at a gym (Building A) and teaching building (Building B) of a university campus in Harbin, China. These buildings were centrally heated, which had fewer window opening periods, hence less influence from outdoor OPEs on indoor levels. All window glasses were pre-cleaned prior to the sampling campaign. The samples were collected with the film growth of 7~77 days in the two buildings. The sampling windows are located in the lobby, and they consist of a row of floor-to-ceiling windows that cannot be opened. When the door is open, air circulates, and the frequency of opening the door in the summer is more than in the winter. Before sampling, Kimwipes (Kimberly Clark, Rosewell, GA) were cleaned by Soxhlet extraction with a mixture solution (1:1, v/v) of acetone and hexane (J.T. Baker, Phillipsburg, NJ). The pre-cleaned Kimwipes were placed in a desiccator for 48 hours and weighed before and after sampling. To avoid contamination, the sampling area (0.5 to 1.5 m^2) was 10 cm away from the window frame. The pre-cleaned Kimwipes were wetted with ethanol and wiped three times over the sampling area. The collected sample was placed in a glass jar and kept at –20 °C until analysis. Measurements of indoor temperature and humidity were listed in Table S1.

A known amount of the surrogate standards comprising tri-n-butyl phosphate-D_{27} (TNBP-D_{27}) and TPHP-D_{15} (Chiron AS, Norway) was injected into the film sample

before extraction. The sample was extracted three times with a mixture of 40 mL acetone and dichloromethane (1:1 v.v., J.T. Baker, Phillipsburg, NJ) by shaking, then concentrated to 1 mL using a rotary evaporator and nitrogen blowdown. Finally, isooctane (1.0 mL) (J.T. Baker, Phillipsburg, NJ) was added as a keeper solvent.

The instrument method was described in the previous literature (Sun et al., 2019). Details of the 12 target compounds are provided in Table S2. In summary, the target OPEs in the indoor window film samples were separated on a DB-5MS column (30 m × 0.25 mm × 0.25 um, J&W Scientific) employing split-less injection using an Agilent 6890 series gas chromatography system with a model 5975B mass selective detector. The oven program started at 90 ℃, held for 1.25 min, then escalated by 10 ℃/min to 240 ℃, then 20 ℃/min to 310 ℃, held for 16 min.

2.2. Quality assurance and quality control

Eight indoor window film samples were treated in batches, along with two procedural blanks and two procedure spikes. Procedural blanks were brought to the sampling site, exposed to air during sampling, and treated as actual samples. tri-iso-propyl phosphate (TIPP), tripropyl phosphate (TPrP), tripentyl phosphate (TPeP), and TDCPP were not detected in procedural blanks (n = 16), whereas the other OPEs were found at low levels (Table S3). The average procedure blanks values were used to blank-correct the final concentrations of OPEs in window film samples. Spike recovery rates ranged from 71% to 113% on average. The average surrogate recovery varied from 74% to 94%, which was considered acceptable. Hence the OPE concentrations were not modified for

recovery. The method detection limit (MDL) was calculated using the mean blank value plus three times the standard deviation (Table S3). If no OPE was found in the blanks, the MDL was substituted with the instrument detection limit (IDL), which was specified as the signal-to-noise ratio of 10:1. If the concentrations were lower than MDL, a value of half MDL was applied. The data was statistically analyzed using the SPSS statistical program (version 22.0). Furthermore, the statistical analysis was performed on the analytes with a detection frequency > 50%.

Concentrations of OPEs can be calculated by dividing the mass of OPEs by the sampling area (ng/m^2 film), the weight of window film (μg/g film), and the volume of window films (g/m^3 film), respectively. The mass of the window film sample was calculated by weighing the mass of the Kimwipe before and after sampling conditioned at constant temperature and humidity. The volume of the film was calculated by multiplying the sample area by the thickness of the film, which is estimated using equation S6 in Text S2 in SI.

2.3. Calculation of the equilibrium time between window film and air

Terzaghi et al. converted outdoor window film to atmospheric PAH concentrations (Terzaghi et al., 2015). Here, a similar procedure is applied to estimate the indoor air concentrations of OPEs by using the film concentrations. In general, a chemical (such as OPE) uptake by a PAS (such as indoor window film) is initially linear, then enters the curve phase, and finally reaches equilibrium between sorbing medium and air (Shoeib and Harner 2002). The sampling times (t) taken to achieve 25% (t_{25}) and 95%

(t_{95}) of the conditions of equilibrium between window film and indoor air indicate different stages of uptake for the chemical, i.e., the equilibrium phase when $t \geq t_{95}$, the curvilinear stage when $t_{25} < t < t_{95}$, and the linear uptake region if $t \leq t_{25}$. Values of t_{25} and t_{95} can be further calculated by $0.29/k_U$ and $3/k_U$, respectively, where k_U is the rate constant for uptake (h^{-1}). The value of k_U was calculated using the following equation (Shoeib and Harner 2002, Csiszar et al., 2012, Wang et al., 2017, Yang et al., 2018),

$$k_U = k_A / (K_{F-A} \times \delta_{bulk}) \quad (1)$$

where k_A is the air-side mass transfer coefficient (m/h) which varies with wind speeds (Diamond et al., 2001), the length of the surface in the direction of the wind (Diamond et al., 2001), and chemical molecular weight (MW) (Terzaghi et al., 2015) (For more details see SI, Text S1), δ_{bulk} is the thickness of the window film (m), and $K_{F\text{-}A}$ is the partition coefficient of film-air (dimensionless) which was derived from partition coefficient of octanol-air (K_{OA}) as follows (Csiszar et al., 2012),

$$\log K_{F-A} = 1.1 \times \log K_{OA} - 0.54 \quad (2)$$

and $\log K_{OA}$ can be calculated as (Wang et al., 2017),

$$\log K_{OA} = A + B/T \quad (3)$$

where the value of intercepts (A) and slope (B) are listed in Table S2, T is the temperature (K) at the time of sampling.

2.4. Conversion of gas-phase OPE concentration

When the airborne phase and film phase has reached equilibrium conditions, the

concentrations of gas-phase OPEs can be estimated using the following equation (Genualdi and Harner 2012, Terzaghi et al., 2015):

$$C_A = C_F / K_{F-A} \quad (4)$$

where C_A is the concentration of OPEs in gas phase air (ng/m^3 air), C_F is the concentration of OPEs in the window film (ng/m^3 film), and $K_{F\text{-}A}$ is given by Equation (2).

When equilibrium was not reached, the concentration of gas-phase OPEs was estimated using the following equation (Genualdi and Harner 2012, Terzaghi et al., 2015),

$$C_A = C_F / K_{F-A} \times (1\text{-}\ \exp\text{-}\ (k_A / \delta_{bulk} K_{F-A}) \times t) \quad (5)$$

where t is the sampling time (h).

3. Results and discussion

3.1. The concentrations of OPEs in the indoor window films

There are three expressions of the concentrations of OPEs in window film, including mass per unit area (ng/m^2 film), mass per unit volume (g/m^3 film), and mass per unit film mass (μg/g film). The mass per unit area reflects the total amount of OPEs accumulated on the film throughout the exposure time. In contrast, the mass per unit film mass reflects the concentrations of OPEs associated with available window film. The concentrations of OPEs in window films are summarized in Table 1 (ng/m^2), Table S4a (μg/g), and Table S4b (g/m^3). The area-normalized concentration and fraction of OPEs

222 are shown in Fig. S1 and Fig. S2, respectively. Except for TIPP and TPeP, which were
223 not found in any samples and are thus removed from the following discussion, most
224 OPEs showed high detection frequencies ranging between 71% and 100%.

225 In winter, the dominant OPEs was TCEP, with median value of 18.1 ng/m^2 (4.31 μg/g),
226 accounting for 15% of OPEs, followed by TPHP (14.8 ng/m^2, 3.16 μg/g, 13%) and TCPP
227 (14.2 ng/m^2, 3.16 μg/g, 12%). TCEP and TCPP are widely used as flame retardants in
228 industrial and household products, such as automobile accessories, electronic devices,
229 upholstery foam, bed mattresses, and toys (Zhang et al., 2016, Chen et al., 2019). TCEP
230 and TCPP are chlorinated OPEs that were proposed to be more persistent than non-
231 chlorinated OPEs (Suhring et al., 2016). The winter compositional profile of OPEs is
232 comparable to that of skin wipes (Liu et al., 2017), suspended particulate matter (Yang
233 et al., 2014), and dormitory dust (Sun et al., 2019).

234 In summer, the composition of OPEs differed from that of winter (Fig. S2), showing
235 that TNBP was the most abundant OPEs with a median value of 18.9 ng/m^2 (3.81 μg/g,
236 20%) in summer, followed by TCEP (10.5 ng/m^2, 3.33 μg/g, 18%) and tris(2-
237 butoxyethyl) phosphate (TBEP) (10.1 ng/m^2, 2.30 μg/g, 12%). As most non-halogenated
238 OPEs, TNBP and TBEP are employed as plasticizers and lubricants, as well as flame
239 retardants for plastics, rubber, and foam (Salamova et al., 2013). Chlorinated OPEs
240 (TCEP, TCPP, TDCPP) account for 36% and 30% of the total OPEs in winter and
241 summer, respectively. TCEP was the most prevalent chlorinated OPEs, accounting for
242 almost 48% and 44% of the total chlorinated OPEs in winter and summer, respectively.

Since these are indoor samples, this seasonal difference could be due to the differentiated evaporation (from sources) and partition of the window films at different temperatures.

An overview of the recently published literature on OPEs is presented in Table S5. The extremely high concentrations of TCEP, TCPP, and TDCPP (927 ng/m^2, 1740 ng/m^2, and 25300 ng/m^2, respectively) were found in gymnastics studios before removing foam blocks (Ceballos et al., 2018). Compared to the profile of this study, TDCPP was generally the dominating chlorinated OPEs in gymnastics studios (Ceballos et al., 2018), and in homes from the USA and the Czech Republic, and Canada (Vykoukalova et al., 2017). The concentration of TDCPP in gymnastics studios was higher than in this study, which could be due to TDCPP being used in PUF (La Guardia and Hale, 2015). In addition, TCPP was the most abundant compound in the home in the Czech Republic (Vykoukalova et al., 2017) and Beijing (Lv et al., 2022), and preschool in Sweden (Persson et al., 2018). Furthermore, in the current investigation, the total amounts of all chlorinated OPEs (37.7 and 23.8 ng/m^2 in winter and summer, respectively) were lower than those from households in China (112 ng/m^2) (Li et al., 2019), USA (181 ng/m^2), Canada (153 ng/m^2) and Czech Republic (626 ng/m^2) (Vykoukalova et al., 2017) but higher than preschools in Sweden (9.4 ng/m^2) (Persson et al., 2018). This disparity could be attributed to room type and differences in usage patterns between countries. For non-chlorinated OPEs, concentrations of tri-iso-butyl phosphate (TiBP) (12.7 and 8.76 ng/m^2 in winter and summer, respectively) in the current study were almost ten times lower than the results from the home samples (108 ng/m^2) in the same city (Li et al., 2019),

264 which might be attributed to more furniture and electronics in homes than in campus
265 buildings. The concentrations of TBEP in winter and summer (7.77 and 10.1 ng/m^2,
266 respectively) were up to 300 and 200 times lower than those reported in Li et al (Li et
267 al., 2019). TBEP is typically used for floor polishing and waxing, which were not used
268 in our sampling site. The levels of TNBP in winter and summer (10.9 and 18.9 ng/m^2,
269 respectively) were higher than those observed in Sweden (< 1.4 ng/m^2) and the USA
270 (8.65 ng/m^2), but lower than in Canada (29.8 ng/m^2) and the Czech Republic (72.6
271 ng/m^2). Therefore, the majority of the OPEs determined in this research from campus
272 buildings could be considered lower than those reported in previous studies.

273 Indoor mass-normalized concentrations have been reported for some compounds,
274 such as PBDEs (Li et al., 2010), PAHs (Pan et al., 2012), and polar organic compounds
275 (such as n-alkane and terpene) (Liu et al., 2003). However, as we are aware, data on the
276 mass-normalized concentrations for OPEs in indoor window films have not been
277 reported in the literature. Except for TCPP and TPHP, the mass-normalized
278 concentrations in winter and summer were comparable in this study. The concentrations
279 of OPEs in inner windowsill dust in Guangzhou, China (Tang et al., 2020) were also
280 listed in Table S5, which showed lower concentrations than in this study.

281 *3.2. Accumulation of OPEs in window film*

282 The total area-normalized concentrations of OPEs (ng/m^2) were plotted against the
283 growth day, as shown in Fig. 1A and Fig. 1C. Significant correlations (Pearson
284 correlation $p < 0.05$) were found between the OPE concentrations and the film growth

285 day, with the correlation coefficients (r) of 0.88 and 0.72 for winter and summer,
286 respectively. The increasing linear trends of OPE mass in the sampling area were
287 consistent with that of other classes of chemicals such as PCBs (Wu et al., 2008), PAHs
288 (Pan et al., 2012, Huo et al., 2019), and PAEs (Huo et al., 2016), except for PBDEs (Li
289 et al., 2010).

290 There was limited information about the temporal trends of the mass-normalized
291 concentrations of OPEs in the window film. Fig. 1B and Fig. 1D, for winter and summer,
292 respectively, showed that the mass-normalized concentrations of OPEs (μg/g) decreased
293 over time, but the trends were not significant ($p > 0.05$). This phenomenon occurred
294 because the accumulation of OPEs in the film could be slower than the growth of the
295 window film. In this study, the doubling times of the weight of the window film were
296 estimated at 16-18 days, lower than that of OPE concentrations (ng/m^2) with values of
297 27-28 days. A previous study reported the mass composition of urban window film in
298 downtown Toronto, in which inorganic compounds accounted for almost 94% and
299 organic carbon for approximately 5% (Lam et al., 2005). These urban window films
300 were collected from the outdoor windows, thus quite different from the indoor window
301 films, which have higher organic contents. The mass of OPEs merely occupied a small
302 percentage of the window films, and the disparity between organic contents and
303 inorganic contents increased over time, as shown in Fig. 1B and Fig. 1D. However, it is
304 possible that the mass-normalized concentrations of OPEs did not change much over
305 time.

306 Spearman correlation analysis was carried out between the concentration (ng/m^2) of
307 individual OPE compounds and the influencing parameters, such as the growth days of
308 window film, the film thickness, indoor temperature, and humidity (Table S6). Except
309 for TCEP (r = 0.25, p > 0.05), there were significant correlations between the log-
310 transformed concentration (ng/m^2) of individual OPE and the growth days of window
311 film (r > 0.50, p < 0.01). Other than TiBP, TNBP, and TCEP, the remaining OPEs have
312 shown positive associations between the concentrations and the thickness of the window
313 film (p < 0.05 or p < 0.01). There were positive and significant correlations between
314 indoor temperature and concentrations of two OPEs, i.e. TPrP (r = 0.44, p < 0.05) and
315 TDCPP (r = 0.48, p < 0.05). Furthermore, negative and significant correlations between
316 indoor humidity and concentrations of three OPEs were discovered: TNBP (r = -0.42, p
317 < 0.05), TDCPP (r = -0.53, p < 0.01) and 2-ethylhexyl diphenyl phosphate (EHDPP)(r
318 = -0.53, p < 0.01). This phenomenon suggests that moisture in the film may impact the
319 equilibrium behaviors of OPEs. In general, the area-normalized concentrations of the
320 majority of OPEs in window film exhibited linear growth patterns that were strongly
321 influenced by the film growth time, followed by the film thickness.

322 Significant differences were found when the concentrations of TNBP, TCPP, and
323 TPHP were compared between winter and summer (Mann-Whitney test, p < 0.01).
324 Accordingly, the studied OPEs can be classified into two groups. The first group
325 includes TCPP and TPHP with significantly higher (p < 0.05) concentrations (14.2 and
326 14.8 ng/m^2) in winter than those in summer (4.60 and 3.74 ng/m^2). This significant

difference could be attributed to the higher concentrations of TCPP and TPHP in the indoor environment due to poorly ventilated circumstances during the cold winter period in Northeast China. All other OPEs are in the second group, which had lower concentrations in winter than in summer. For example, TNBP had a significantly lower concentration in winter (10.9 ng/m^2) than in summer (18.9 ng/m^2). According to Wong et al., several OPEs, including TNBP, in outdoor air have seasonal features, with concentrations increasing with ambient temperature (Wong et al., 2018). Therefore, it is reasonable to conclude that more frequent ventilation and higher temperatures in summer than in winter have made outdoor air a significant source of some OPEs to the indoor window film, resulting in higher TNBP concentrations in summer than in winter.

EHDPP was the only compound that significantly differed between the two buildings. The concentration of EHDPP with the median value of 10.5 ng/m^2 was higher in building A than that in building B (6.12 ng/m^2). EHDPP is widely utilized as a plasticizer and flame retardant in a variety of products, including Polyvinyl chloride (PVC), rubber, and food packaging (Shen et al., 2019). Therefore, we speculated that the emissions from numerous fitness equipment which were made of PVC materials in building A were the primary reasons for this variation. The upper and bottom window film samples did not differ significantly. Furthermore, a significant difference in TCEP and TPHP concentrations and temperature during wintertime was identified in different orientations of the windows in building B, which may be related to photodegradation (Bollmann et al., 2012). In conclusion, indoor temperature, humidity, ventilation,

photodegradation, the presence of fitness equipment, and seasonal fluctuations all influenced the levels of the majority of OPEs in the window films.

3.3. Equilibrium time between window film and air

Based on equation (1) - (3), t_{95} of each OPE under each sampling event in winter (7 sampling times) and summer (11 sampling times) are shown in Fig. 2 and Table S7. If t_{95} is lower than sample time (t), OPE levels in window film have reached equilibrium within the sampling time. TPrP, TiBP, TNBP, and TCEP levels reached equilibrium during each sampling event in winter (Fig. 2a and Table S7). On the other hand, the t_{95} values of TBEP, EHDPP, and TEHP were higher than all sample times, indicating that these compounds remained in the active uptake phase throughout the sampling periods. TDCPP and TPHP can only reach equilibrium in building A during the fifth week (sample ID: W-A-L05), with t_{95} values of 523 hours and 747 hours, respectively, shorter than the sampling time (5 weeks = 840 hours). It is worth noting that the sample W-A-L05 had a film thickness of 1.8 nm and an indoor temperature of 298.15 k (25°C). When all other factors remained constant, thinner film thickness and higher temperature for this sample resulted in a small value of t_{95}, according to equations (1) to (3). For TCPP, some occasional equilibrium can be observed with different sampling times.

For summer samples, TPrP, TiBP, TNBP, and TCEP had reached equilibrium within each sampling time which was consistent with that of winter. Levels of TCPP had reached equilibrium at all sampling sites (Fig. 2b and Table S7), which were slightly inconsistent with that of winter. TDCPP, TBEP, TPHP, EHDPP, and TEHP reminded at

equilibrium conditions for a few sampling points during the summer, which may be attributed to the lower film thickness and higher temperature during those sampling events. For TPrP, TiBP, TNBP, and TCEP in both winter and summer, the log K_{OA} values were less than 9.28 (TCEP at 276.15K), which was one of the key parameters impacting the equilibrium conditions. In comparison, our findings were consistent with previous studies. It was proposed, for example, that OPEs with log $K_{OA} < 8$ would have reached equilibrium (Vykoukalova et al., 2017). The log K_{OA} of PAHs < 12 reached equilibrium by 11 weeks (Huo et al., 2019). PCB28 (log $K_{OA} = 7.86$) and PCB180 (log $K_{OA} = 10.2$) approached equilibrium within hours and days, respectively (Csiszar et al., 2012). The compound with log $K_{OA} < 8$ in 100 nm ethylene vinyl acetate (EVA) synthetic film practically soon reaches equilibrate conditions (Genualdi and Harner 2012).

Because the equilibrium times of OPEs were significantly influenced by the film thickness, it is essential to model the growth of film thickness and to understand the relationship between the equilibrium times of OPEs and the film thickness, as described in Text S2. Generally, the film thickness obtained in this study was comparable with that obtained from the multicomponent partitioning model (Weschler and Nazaroff, 2017) and other studies (Liu et al., 2003, Li et al., 2010). Fig. 3 depicts log K_{OA} of OPEs as a function of film growth rate when the equilibrium conditions are reached based on equations 1-2, which suggests that the equilibrium can be reached for higher log K_{OA} OPEs at a slower film growth rate. As the film growth rate increased, a lower log K_{OA} value would be required to reach equilibrium. For a compound to reach equilibrium

would require the log K_{OA} to be less than 10.85 for a higher film growth rate (> 0.50 nm/day). For the lower film growth rate (0.01 nm/day), the log K_{OA} should be less than 12.39 to reach equilibrium. Mann−Whitney test suggested that no significant difference was observed in film growth rate during winter and summer with the values of 0.13 ± 0.07 and 0.12 ± 0.06 nm/day, respectively (p = 0.85). Under this circumstance, OPEs with log K_{OA} less than 11.5 can reach equilibrium between indoor window film and air.

3.4. Uncertainty and sensitivity analysis of equilibrium time

Based on the foregoing discussion, it was concluded that the equilibrium condition between window film and indoor air was strongly affected by the film thickness and log K_{OA} of the OPEs. When predicting the equilibrium time for specific OPEs, there were uncertainties related to film thickness growth and changes in the indoor environment, such as temperature. To the best of our knowledge, no studies had evaluated the uncertainty and sensitivity of these parameters on the equilibrium time of OPEs in the window film based on the Monto Carlo simulation.

From equation (1)-(3) and equation (S1)-(S3), the equilibrium time was associated with temperature and film thickness. These data were used as the inputs to perform the Monto Carlo simulation (Fig. S3 to Fig. S5). Briefly, all targeted OPEs were divided into two groups. Group 1 includes TPrP, TiBP, TNBP, and TCEP which have lower MW and low log K_{OA} [224 (TPrP) < MW < 286 (TCEP) and 6.5 (TPrP, calculated at 26℃) < log K_{OA} < 9.3 (TCEP, at 3℃)], while Group 2 contains the remain compounds (TCPP, TDCPP, TBEP, TPHP, EHDPP, and TEHP [328 (TCPP) < MW < 435 (TEHP) and 9.6

411 (TCPP, at 26℃) < log K_{OA} < 13.0 (TEHP, at 3℃)]. According to Fig. S3, the degree of
412 uncertainty for temperature and thickness to the equilibrium time can be evaluated. For
413 example, the film thickness was the most sensitive parameter for Group 1, which
414 contributed to a variance between 52% and 60%. Differently, the most uncertain input
415 was the ambient temperature for Group 2, which contributed to 53–63% of the variance.
416 As shown in Fig. S4, the correlation coefficients between each input and the equilibrium
417 time were carried out by the Monte Carlo Simulation. For Group 1, the temperature was
418 the most influential input, with the correlation coefficients ranging between 0.61 and
419 0.67. However, the film thickness posed the most sensitive influence on the equilibrium
420 time in Group 2, with the correlation coefficients in the range of -0.47 to -0.50. The film
421 thickness positively correlated with the model output, while the temperature showed a
422 negative correlation. The uncertainty to the equilibrium time for temperature and
423 thickness with one standard deviation (± SD) change was shown in Fig. S5. Huge
424 changes in equilibrium time were observed for Group 2, suggesting that the equilibrium
425 time of the OPEs with higher log K_{OA} and MW was strongly affected by small changes
426 in the film thickness and indoor temperature.

427 Furthermore, based on equations (1) - (3) and S1-S3, equilibrium time can also be
428 determined by the air-side mass transfer coefficient (k_A, m/h), temperature, and window
429 film thickness. Meanwhile, k_A was calculated using wind speeds (Harner et al., 2003,
430 Cousins 2012, Pan et al., 2018) (the wind speed values from the published paper are
431 listed in Table S8), length of the passive sampler, and chemical MW. In other words,

how the temperature, window film thickness, and wind speed affected the output and contributed to variance can be evaluated through the Monto Carlo simulation (Fig. S6 to Fig. S8). As shown in Fig. S6, the wind speed, thickness, and temperature almost each accounted for one-third contribution to the whole output in Group 1. The wind speed was the most sensitive variable among the three inputs, contributing to 40% of the total variance, followed by indoor temperature (32% - 39%) and film thickness (30% - 33%). For Group 2, the most uncertain input was the temperature which contributed to 56– 64% of the variance, followed by the wind speed and thickness. The correlation coefficients among the three inputs and the equilibrium time are shown in Fig. S7. It should be pointed out that the film thickness was the most sensitive input in Group 1, with the correlation coefficients ranging from 0.38 to 0.42, followed by indoor temperature and wind speed.

Meanwhile, the thickness showed positive correlations with the equilibrium time, while temperature and wind speed showed negative correlations for the whole output. The uncertainty for each input with one standard deviation (±SD) change to the equilibrium time is shown in Fig. S8. A similar statement can be made that the equilibrium time for OPEs with higher log K_{OA} and MW was more sensitive to a slight change in wind speed, thickness, and temperature.

3.5. Conversion of air concentration based on the theoretical approach

First, it was determined whether the targeted OPEs had reached the equilibrium stage ($t \geq t_{95}$, $t_{95}=3/k_U$) using Equations 1-3 and S1-S3. A detailed description of the

453 equilibrium times is available in Table S7. And then, the gas-phase concentrations can
454 be calculated using Equation 4 (equilibrium) or 5 (non-equilibrium) from the volume-
455 normalized concentrations in the film (g/m^3, see Fig. S4b). The predicted gas-phase
456 concentrations (PECs) of OPEs are listed in Table S9**,** along with the vapor-phase OPE
457 concentrations from other literature. The estimated concentrations of TPrP, TiBP, TNBP,
458 and TCEP were lower in winter than in summer, which is reasonable as levels of these
459 lower MW OPEs in the air are sensitive to ambient temperature (Wong et al., 2018). For
460 the remaining OPEs, the concentrations in winter were comparable to those in summer.

461 Compared to the OPEs concentrations captured by PASs in other published literature,
462 the predicted concentrations of TnBP and TCEP in summer were consistent with those
463 measured in the United States, Canada, and the Czech Republic (Vykoukalova et al.,
464 2017). The predicted values of TPHP, EHDPP, and TEHP in both winter and summer
465 were one order of magnitude lower than the measured concentrations from the United
466 States, Canada, and Czech Republic (Vykoukalova et al., 2017), and China (Li et al.,
467 2019). In comparison, EHDPP and TEHP were not detected in those papers which use
468 active samplers (Bergh et al., 2011, Bergh et al., 2011, Luongo and Ostman, 2016, Xu
469 et al., 2016, Tao et al., 2019). Concentrations of TiBP, TNBP, and TCEP in this study
470 were comparable with the values from Sweden (Bergh et al., 2011, Bergh et al., 2011,
471 Luongo and Ostman, 2016, Tao et al., 2019) and Norway (Xu et al., 2016).

472 Since the window film lacks the corresponding gas-phase OPE concentrations in this
473 study, paired data on window film and passive air from the previous study (Vykoukalova

et al., 2017) was selected to verify whether the theoretical approach is suitable for the conversion of OPE concentrations from the window film to gas-phase air. Detailed information about the concentrations, equilibrium time, film thickness, temperature, et cetera is provided in Text S3**.** Briefly, passive air and indoor window film samples (63 paired) in the same room were collected simultaneously for OPEs for 28 days in the Czech Republic, the United States, and Canada in 2013 (Vykoukalova et al., 2017). As shown in Table S10, only TNBP, TCEP, and TCPP have reached the equilibrium state within 28 days.

The PEC was compared with the measured air concentration (MC) using PUF-PAS (Vykoukalova et al., 2017). As shown in Fig. S9, the PEC of TNBP and TCEP were nearly all higher than MC, with the ratio of PEC to EC ranging from 0.75 to 30. The PECs of the remaining OPEs were lower than the MC, with the ratio in the range of 0.01-0.37. The relationship between PEC/MC, MW, and log K_{OA} (Fig. S11) shows that the ratios of PEC to EC were greater than 1 when the log K_{OA} ranged from 8 to 9 and MW ranged from 260 to 290. Nevertheless, when the log K_{OA} is in the range of 9-12 and MW is in the range of 320-440, the ratio of PEC to EC is less than 1.

To summarize, indoor window film could be a PAS for quantitative analysis of some OPEs in the indoor air. Meanwhile, the use of window film to quantify gas-phase OPE concentrations can also lead to the overestimation of lower MW OPEs. There are probably several reasons for this result. The overestimation of gas-phase concentrations for lower MW OPEs could be because these lower MW OPEs can reach equilibrium

much faster than the sampling time of the PUF-PASs. As discussed in the above section, the equilibrium time varies by the selection of parameters, such as temperature, wind speed, log $K_{F\text{-}A,}$ and the window film thickness, which further affects the PECs. For example, from equation 5 (non-equilibrium state), temperature and film thickness both influence the predicted air concentrations. A universal (average) sampling rate was applied in the previous study for all OPEs because of the lack of sampling rates for certain OPEs (Vykoukalova et al., 2017). Therefore, using the same sampling rate without considering the equilibrium conditions creates uncertainty in determining the collected air volume for PUF-PAS, which affects the calculated OPE concentrations (MC) in the indoor air.

4. Limitations and implications

There were several limitations of this study. First, this study lacks sampling of gas-phase concentrations to evaluate the theoretical approach; instead, previously published data were used, but a concurrent sampling of the gas phase with the indoor films would provide more accurate estimates of the concentrations. There were uncertainties associated with PASs as they capture both gas-phase and particle-phase compounds. Second, as the Monte Carlo analysis identified, there was uncertainty in determining the time to equilibrium for high MW OPEs for different temperatures and film thickness. Therefore, accurate measurements of temperature and film thickness are required to determine equilibrium conditions for high MW OPEs. Third, the equilibrium status of the chemicals depends on the film development and the physical-chemical properties of

OPEs. Therefore, the time to equilibrium was only calculated at the time of sampling with a specific film thickness, suggesting that equilibrium conditions were different at different sampling times.

We used the theoretical approach to convert the levels of OPEs in the indoor window film into gas-phase concentrations. It is the first time that the equilibrium time of OPEs between indoor window film and air was estimated in combination with uncertainty and sensitivity analysis. Since indoor window film is very common, it could become a convenient and economical passive sampler for future studies. Under the circumstance of increasing usage and emissions of OPEs, most lower MW OPEs will stay in the indoor air because of their short equilibrium time. With the film growth rate of 0.10 nm/day, OPEs with log K_{OA} greater than 11.5 would keep accumulating onto the indoor surfaces. The study of the equilibrium condition of OPEs reveals the different fates of OPEs in the indoor environment, which helps better understand the fate and transport of OPEs indoors.

Declaration of competing interest

The authors declare that they have no known competing financial interests or personal relationships that could have appeared to influence the work reported in this paper.

Acknowledgements

This work was supported by the State Key Laboratory of Urban Water Resource and Environment, Harbin Institute of Technology (2016TS04). This study was also partially

supported by the Fundamental Scientific Research Funds for Heilongjiang Provincial Institutes, China (CZKYF2020C024) and the National Natural Science Foundation of China (No. 41705105).

Appendix A. Supplementary data

Supplementary data to this article can be found online at https://doi.org/10.1016/.

References

Bergh, C., Aberg, K. M., Svartengren, M., Emenius, G. and Ostman, C., 2011. Organophosphate and phthalate esters in indoor air: a comparison between multi-storey buildings with high and low prevalence of sick building symptoms. *J. Environ. Monit.* 13(7), 2001-2009.

Bergh, C., Torgrip, R., Emenius, G. and Ostman, C., 2011. Organophosphate and phthalate esters in air and settled dust - a multi-location indoor study. *Indoor Air* 21(1), 67-76.

Bollmann, U. E., Moler, A., Xie, Z. Y., Ebinghaus, R. and Einax, J. W., 2012. Occurrence and fate of organophosphorus flame retardants and plasticizers in coastal and marine surface waters. *Water Res.* 46(2), 531-538.

Ceballos, D. M., Broadwater, K., Page, E., Croteau, G. and La Guardia, M. J., 2018. Occupational exposure to polybrominated diphenyl ethers (PBDEs) and other flame retardant foam additives at gymnastics studios: Before, during and after the replacement of pit foam with PBDE-free foams. *Environ. Int.* 116, 1-9.

Cetin, B. and Odabasi, M., 2011. Polybrominated diphenyl ethers (PBDEs) in indoor and outdoor window organic films in Izmir, Turkey. *J. Hazard. Mater.* 185(2-3), 784-791.

Chen, Y., Zhang, Q., Luo, T., Xing, L. and Xu, H., 2019. Occurrence, distribution and health risk

assessment of organophosphate esters in outdoor dust in Nanjing, China: Urban vs. rural areas. *Chemosphere* 231, 41-50.

Cousins, A. P., 2012. The effect of the indoor environment on the fate of organic chemicals in the urban landscape. *Sci. Total Environ.* 438, 233-241.

Csiszar, S. A., Diamond, M. L. and Thibodeaux, L. J., 2012. Modeling urban films using a dynamic multimedia fugacity model. *Chemosphere* 87(9), 1024-1031.

Diamond, M. L., Priemer, D. A. and Law, N. L., 2001. Developing a multimedia model of chemical dynamics in an urban area. *Chemosphere* 44(7), 1655-1667.

Genualdi, S. and Harner, T., 2012. Rapidly Equilibrating Micrometer Film Sampler for Priority Pollutants in Air. *Environ. Sci. Technol.* 46(14), 7661-7668.

Greaves, A. K. and Letcher, R. J., 2017. A Review of Organophosphate Esters in the Environment from Biological Effects to Distribution and Fate. *Bull. Environ. Contam. Toxicol.* 98(1), 2-7.

Hallanger, I. G., Sagerup, K., Evenset, A., Kovacs, K. M., Leonards, P., Fuglei, E., Routti, H., Aars, J., Strom, H., Lydersen, C. and Gabrielsen, G. W., 2015. Organophosphorous flame retardants in biota from Svalbard, Norway. *Mar. Pollut. Bull.* 101(1), 442-447.

Harner, T., Farrar, N. J., Shoeib, M., Jones, K. C. and Gobas, F. A. P. C., 2003. Characterization of polymer-coated glass as a passive air sampler for persistent organic pollutants. *Environ. Sci. Technol.* 37(11), 2486-2493.

Hu, M. Y., Li, J., Zhang, B. B., Cui, Q. L., Wei, S. and Yu, H. X., 2014. Regional distribution of halogenated organophosphate flame retardants in seawater samples from three coastal cities in China. *Mar. Pollut. Bull.* 86(1-2), 569-574.

578 Huo, C. Y., Liu, L. Y., Zhang, Z. F., Ma, W. L., Song, W. W., Li, H. L., Li, W. L., Kannan, K., Wu, Y. K.,
579 Han, Y. M., Peng, Z. X. and Li, Y. F., 2016. Phthalate Esters in Indoor Window Films in a
580 Northeastern Chinese Urban Center: Film Growth and Implications for Human Exposure. *Environ.*
581 *Sci. Technol.* 50(14), 7743-7751.
582 Huo, C. Y., Sun, Y., Liu, L. Y., Sverko, E., Li, Y. F., Li, W. L., Ma, W. L., Zhang, Z. F. and Song, W. W.,
583 2019. Assessment of human indoor exposure to PAHs during the heating and non-heating season:
584 Role of window films as passive air samplers. *Sci. Total Environ.* 659, 293-301.
585 Kemmlein, S., Hahn, O. and Jann, O., 2003. Emissions of organophosphate and brominated flame
586 retardants from selected consumer products and building materials. *Atmos. Environ.* 37(39-40), 5485-
587 5493.
588 Kim, J. W., Isobe, T., Muto, M., Tue, N. M., Katsura, K., Malarvannan, G., Sudaryanto, A., Chang, K. H.,
589 Prudente, M., Viet, P. H., Takahashi, S. and Tanabe, S., 2014. Organophosphorus flame retardants
590 (PFRs) in human breast milk from several Asian countries. *Chemosphere* 116, 91-97.
591 Kim, U. J., Wang, Y., Li, W. and Kannan, K., 2019. Occurrence of and human exposure to organophosphate
592 flame retardants/plasticizers in indoor air and dust from various microenvironments in the United
593 States. *Environ. Int.* 125, 342-349.
594 La Guardia, M. J. and Hale, R. C., 2015. Halogenated flame-retardant concentrations in settled dust,
595 respirable and inhalable particulates and polyurethane foam at gymnastic training facilities and
596 residences. *Environ. Int.* 79, 106-114.
597 Lam, B., Diamond, M. L., Simpson, A. J., Makar, P. A., Truong, J. and Hernandez-Martinez, N. A., 2005.
598 Chemical composition of surface films on glass windows and implications for atmospheric chemistry.

Atmos. Environ. 39(35), 6578-6586.

Li, H. L., Liu, L. Y., Zhang, Z. F., Ma, W. L., Sverko, E., Zhang, Z., Song, W. W., Sun, Y. and Li, Y. F., 2019. Semi-volatile organic compounds in infant homes: Levels, influence factors, partitioning, and implications for human exposure. *Environ. Pollut.* 251, 609-618.

Li, J., Lin, T. A., Pan, S. H., Xu, Y., Liu, X. A., Zhang, C. and Li, X. D., 2010. Carbonaceous matter and PBDEs on indoor/outdoor glass window surfaces in Guangzhou and Hong Kong, South China. *Atmos. Environ.* 44(27), 3254-3260.

Li, J., Xie, Z., Mi, W., Lai, S., Tian, C., Emeis, K. C. and Ebinghaus, R., 2017. Organophosphate Esters in Air, Snow, and Seawater in the North Atlantic and the Arctic. *Environ. Sci. Technol.* 51(12), 6887-6896.

Liu, Q. T., Chen, R., McCarry, B. E., Diamond, M. L. and Bahavar, B., 2003. Characterization of polar organic compounds in the organic film on indoor and outdoor glass windows. *Environ. Sci. Technol.* 37(11), 2340-2349.

Liu, X., Yu, G., Cao, Z., Wang, B., Huang, J., Deng, S. and Wang, Y., 2017. Occurrence of organophosphorus flame retardants on skin wipes: Insight into human exposure from dermal absorption. *Environ. Int.* 98, 113-119.

Luongo, G. and Ostman, C., 2016. Organophosphate and phthalate esters in settled dust from apartment buildings in Stockholm. *Indoor Air* 26(3), 414-425.

Lv, K., Bai, L., Song, B., Ma, X., Hou, M., Fu, J., Shi, Y., Wang, Y. and Jiang, G., 2022. Presence of organophosphate flame retardants (OPEs) in different functional areas in residential homes in Beijing, China. *J Environ Sci-China* 115, 277-285.

Meeker, J. D. and Stapleton, H. M., 2010. House Dust Concentrations of Organophosphate Flame Retardants in Relation to Hormone Levels and Semen Quality Parameters. *Environ. Health Perspect.* 118(3), 318-323.

Mitra, S. and Ray, B., 1995. Patterns and sources of polycyclic aromatic hydrocarbons and their derivatives in indoor air. *Atmos. Environ.* 29(22), 3345-3356.

Ni, Y., Kumagai, K. and Yanagisawa, Y., 2007. Measuring emissions of organophosphate flame retardants using a passive flux sampler. *Atmos. Environ.* 41(15), 3235-3240.

Pan, S.-H., Li, J., Lin, T., Zhang, G., Li, X.-D. and Yin, H., 2012. Polycyclic aromatic hydrocarbons on indoor/outdoor glass window surfaces in Guangzhou and Hong Kong, south China. *Environ. Pollut.* 169, 190-195.

Pan, S., Xiong, Y. Z., Han, Y. Y., Zhang, X. X., Xia, L., Wei, S., Wu, J. S. and Han, M. J., 2018. A study on influential factors of occupant window-opening behavior in an office building in China. *Build. Environ.* 133, 41-50.

Persson, J., Wang, T. and Hagberg, J., 2018. Organophosphate flame retardants and plasticizers in indoor dust, air and window wipes in newly built low-energy preschools. *Sci. Total Environ.* 628-629, 159-168.

Salamova, A., Ma, Y., Venier, M. and Hites, R. A., 2013. High Levels of Organophosphate Flame Retardants in the Great Lakes Atmosphere. *Environ. Sci. Tech. Let.* 1(1), 8-14.

Shen, J., Zhang, Y., Yu, N., Crump, D., Li, J., Su, H., Letcher, R. J. and Su, G., 2019. Organophosphate Ester, 2-Ethylhexyl Diphenyl Phosphate (EHDPP), Elicits Cytotoxic and Transcriptomic Effects in Chicken Embryonic Hepatocytes and Its Biotransformation Profile Compared to Humans. *Environ.*

641 *Sci. Technol.* 53(4), 2151-2160.

642 Shoeib, M. and Harner, T., 2002. Characterization and comparison of three passive air samplers for
643 persistent organic pollutants. *Environ. Sci. Technol.* 36(19), 4142-4151.

644 Shoeib, T., Webster, G. M., Hassan, Y., Tepe, S., Yalcin, M., Turgut, C., Kurt-Karakuş, P. B. and Jantunen,
645 L., 2019. Organophosphate esters in house dust: A comparative study between Canada, Turkey and
646 Egypt. *Sci. Total Environ.* 650, 193-201.

647 Suhring, R., Diamond, M. L., Scheringer, M., Wong, F., Pucko, M., Stern, G., Burt, A., Hung, H., Fellin,
648 P., Li, H. and Jantunen, L. M., 2016. Organophosphate Esters in Canadian Arctic Air: Occurrence,
649 Levels and Trends. *Environ. Sci. Technol.* 50(14), 7409-7415.

650 Sun, Y., Liu, L.-Y., Sverko, E., Li, Y.-F., Li, H.-L., Huo, C.-Y., Ma, W.-L., Song, W.-w. and Zhang, Z.-F.,
651 2019. Organophosphate flame retardants in college dormitory dust of northern Chinese cities:
652 Occurrence, human exposure and risk assessment. *Sci. Total Environ.* 665, 731-738.

653 Tang, B., Christia, C., Malarvannan, G., Liu, Y.-E., Luo, X.-J., Covaci, A., Mai, B.-X. and Poma, G., 2020.
654 Legacy and emerging organophosphorus flame retardants and plasticizers in indoor
655 microenvironments from Guangzhou, South China. *Environ. Int.* 143.

656 Tao, F., Sellström, U. and De Wit, C. A., 2019. Organohalogenated Flame Retardants and
657 Organophosphate Esters in Office Air and Dust from Sweden. *Environ. Sci. Technol.* 53(4), 2124-
658 2133.

659 Terzaghi, E., Scacchi, M., Cerabolini, B., Jones, K. C. and Di Guardo, A., 2015. Estimation of polycyclic
660 aromatic hydrocarbon variability in air using high volume, film, and vegetation as samplers. *Environ.*
661 *Sci. Technol.* 49(9), 5520-5528.

662 Vykoukalova, M., Venier, M., Vojta, S., Melymuk, L., Becanova, J., Romanak, K., Prokes, R., Okeme, J.
663 O., Saini, A., Diamond, M. L. and Klanova, J., 2017. Organophosphate esters flame retardants in the
664 indoor environment. *Environ. Int.* 106, 97-104.
665 Wang, Q. Z., Zhao, H. X., Wang, Y., Xie, Q., Chen, J. W. and Quan, X., 2017. Determination and prediction
666 of octanol-air partition coefficients for organophosphate flame retardants. *Ecotoxicol. Environ. Saf.*
667 145, 283-288.
668 Wei, G. L., Li, D. Q., Zhuo, M. N., Liao, Y. S., Xie, Z. Y., Guo, T. L., Li, J. J., Zhang, S. Y. and Liang, Z.
669 Q., 2015. Organophosphorus flame retardants and plasticizers: Sources, occurrence, toxicity and
670 human exposure. *Environ. Pollut.* 196, 29-46.
671 Weschler, C. J. and Nazaroff, W. W., 2017. Growth of organic films on indoor surfaces. *Indoor Air* 27(6),
672 1101-1112.
673 Wong, F., de Wit, C. A. and Newton, S. R., 2018. Concentrations and variability of organophosphate esters,
674 halogenated flame retardants, and polybrominated diphenyl ethers in indoor and outdoor air in
675 Stockholm, Sweden. *Environ. Pollut.* 240, 514-522.
676 Wu, R. W., Harner, T. and Diamond, M. L., 2008. Evolution rates and PCB content of surface films that
677 develop on impervious urban surfaces. *Atmos. Environ.* 42(24), 6131-6143.
678 Xu, F. C., Giovanoulis, G., van Waes, S., Padilla-Sanchez, J. A., Papadopoulou, E., Magner, J., Haug, L.
679 S., Neels, H. and Covaci, A., 2016. Comprehensive Study of Human External Exposure to
680 Organophosphate Flame Retardants via Air, Dust, and Hand Wipes: The Importance of Sampling and
681 Assessment Strategy. *Environ. Sci. Technol.* 50(14), 7752-7760.
682 Yang, F. X., Ding, J. J., Huang, W., Xie, W. and Liu, W. P., 2014. Particle Size-Specific Distributions and

683 Preliminary Exposure Assessments of Organophosphate Flame Retardants in Office Air Particulate
684 Matter. *Environ. Sci. Technol.* 48(1), 63-70.
685 Yang, M., Li, Y. F., Qiao, L. N. and Zhang, X. M., 2018. Estimating subcooled liquid vapor pressures and
686 octanol-air partition coefficients of polybrominated diphenyl ethers and their temperature
687 dependence. *Sci. Total Environ.* 628-629, 329-337.
688 Zhang, W., Wang, P., Li, Y., Wang, D., Matsiko, J., Yang, R., Sun, H., Hao, Y., Zhang, Q. and Jiang, G.,
689 2019. Spatial and temporal distribution of organophosphate esters in the atmosphere of the Beijing-
690 Tianjin-Hebei region, China. *Environmental pollution (Barking, Essex : 1987)* 244, 182-189.
691 Zhang, W., Zhang, Y., Wang, Z., Xu, T., Huang, C., Yin, W., Wang, J., Xiong, W., Lu, W., Zheng, H. and
692 Yuan, J., 2016. Tris(2-chloroethyl)phosphate-induced cell growth arrest via attenuation of SIRT1-
693 independent PI3K/Akt/mTOR pathway. *J. Appl. Toxicol.* 36(7), 914-924.
694 Zhong, M., Wu, H., Mi, W., Li, F., Ji, C., Ebinghaus, R., Tang, J. and Xie, Z., 2018. Occurrences and
695 distribution characteristics of organophosphate ester flame retardants and plasticizers in the
696 sediments of the Bohai and Yellow Seas, China. *Sci. Total Environ.* 615, 1305-1311.
697
698

Tables and figures

Table 1. The area-normalized concentrations of OPEs (in ng/m^2) in indoor window films.

Compounds	Median	Geomean	25th	75th	DF%	Median	Geomean	25th	75th	DF%
	Winter (n=26)					Summer (n=38)				
TIPP	nd	nd	nd	nd	0	nd	nd	nd	nd	0
TPrP	4.58	3.69	2.16	5.98	100	4.71	3.06	1.14	6.35	71
TiBP	12.6	10.0	5.32	16.8	96	8.76	11.4	4.89	17.9	97
TNBP	10.9	11.5	7.08	21.1	100	18.9	18.1	13.6	25.5	97
TCEP	18.1	18.3	13.8	25.7	100	10.5	14.0	6.91	22.2	97
TCPP	14.2	13.3	9.48	21.4	100	4.60	5.22	2.51	7.80	92
TPeP	nd	nd	nd	nd	0	nd	nd	nd	nd	0
TDCPP	5.34	6.04	4.10	9.43	100	8.69	5.11	1.08	15.2	100
TBEP	7.77	7.92	4.33	12.5	96	10.1	12.1	4.14	24.3	71
TPHP	14.8	14.7	10.5	21.0	100	3.74	4.53	2.42	6.92	100
EHDPP	9.65	9.46	6.71	15.9	100	6.09	7.74	3.90	12.7	92
TEHP	6.95	5.23	3.57	10.8	100	4.30	5.91	3.26	7.87	92
∑OPEs	104	110	80.5	149	83	78.8	103	56.1	181	76

704

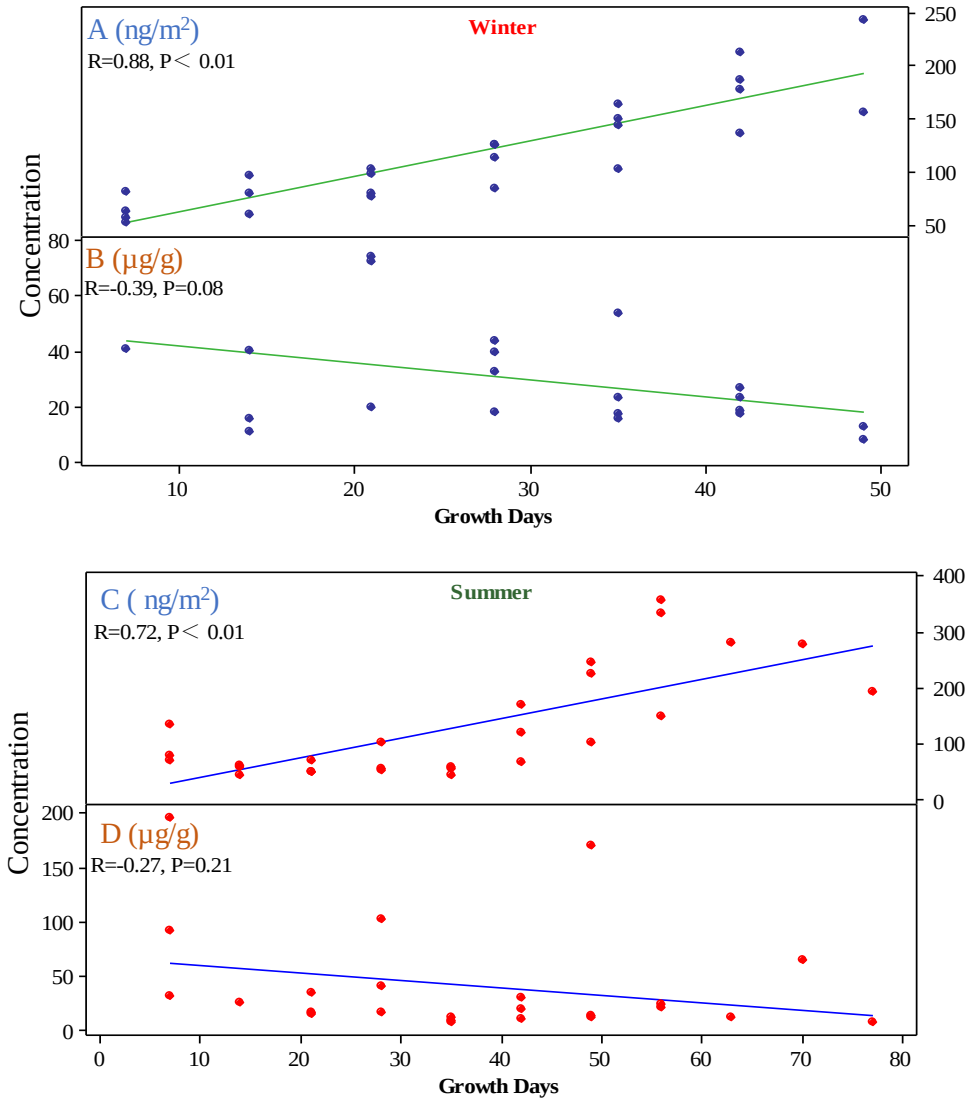

705

706

707 **Fig. 1.** Correlations between concentrations of ∑OPEs (ng/m^2 and μg/g) and the film

708 growth days in winter (A, B) and summer (C, D).

709

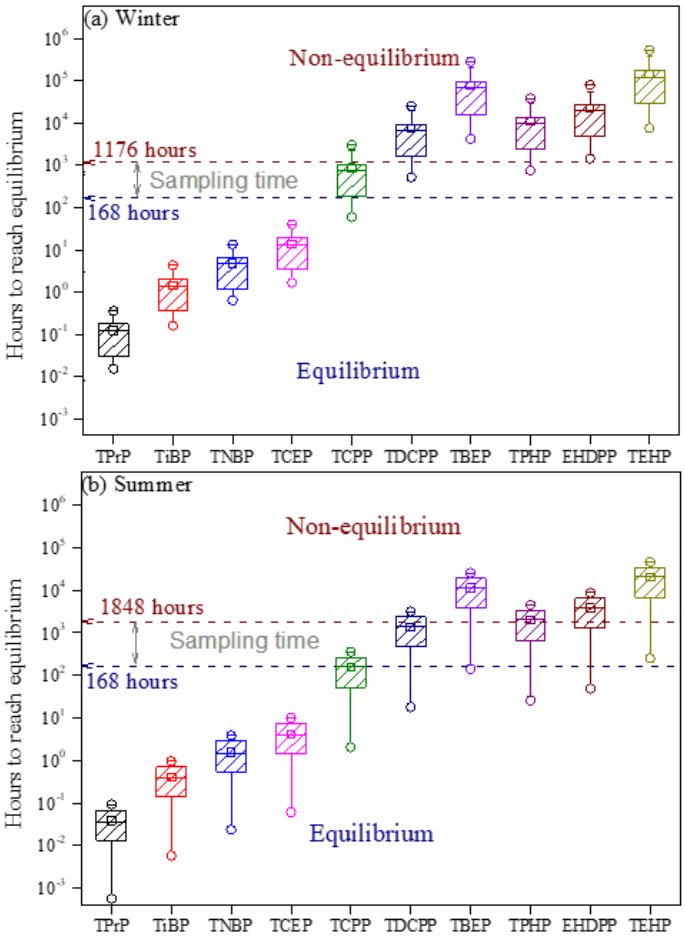

710

711 **Fig. 2.** The time (hour) required to reach the equilibrium state for OPEs in indoor

712 window films collected in winter (a) and summer (b).

713

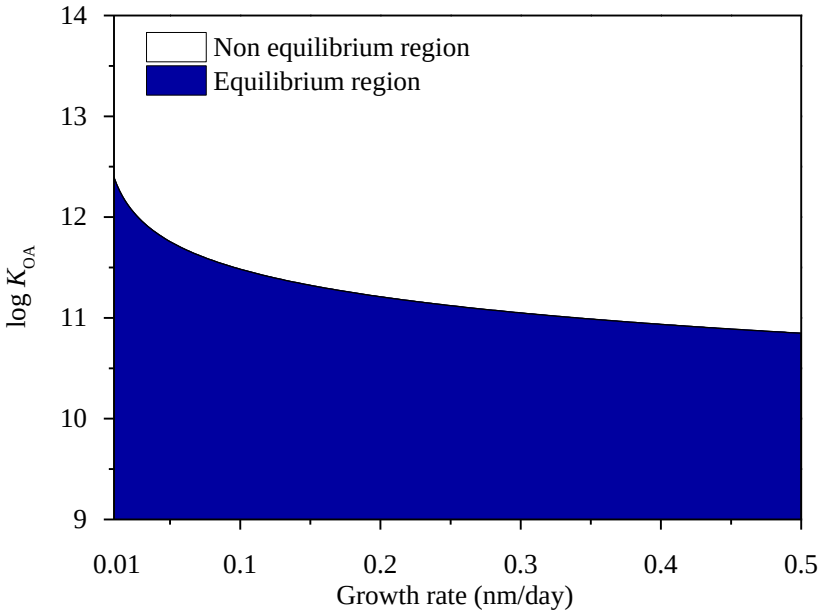

714

715 **Fig. 3.** Modeling equilibrium regions for the log K_{OA} of OPEs as a function of film

716 growth rate.